HHS Public Access

Author manuscript

ACS Chem Biol. Author manuscript; available in PMC 2019 May 07.

Published in final edited form as:

ACS Chem Biol. 2016 December 16; 11(12): 3461–3472. doi:10.1021/acschembio.6b00902.

A Malaria Transmission-Blocking (+)-Usnic Acid Derivative Prevents *Plasmodium* Zygote-to-Ookinete Maturation in the Mosquito Midgut

Rebecca Pastrana-Mena[†,∇], **Derrick K. Mathias**[†,∇,‖], **Michael Delves**[‡], **Krithika Rajaram**[†], **Jonas G. King**[†,⊥], **Rebecca Yee**[†], **Beatrice Trucchi**[§], **Luisella Verotta**[§], and **Rhoel R. Dinglasan**[*,†,#]

[†]W. Harry Feinstone Department of Molecular Microbiology and Immunology, Malaria Research Institute, Johns Hopkins Bloomberg School of Public Health, Baltimore, Maryland, United States

[‡]Department of Life Sciences, Imperial College of London, London, United Kingdom

[§]Department of Chemistry, University of Milan, Milan, Italy

Abstract

The evolution of drug resistance is a recurrent problem that has plagued efforts to treat and control malaria. Recent emergence of artemisinin resistance in Southeast Asia underscores the need to develop novel antimalarials and identify new targetable pathways in *Plasmodium* parasites. Transmission-blocking approaches, which typically target gametocytes in the host bloodstream or parasite stages in the mosquito gut, are recognized collectively as a strategy that when used in combination with antimalarials that target erythrocytic stages will not only cure malaria but will also prevent subsequent transmission. We tested four derivatives of (+)-usnic acid, a metabolite isolated from lichens, for transmission-blocking activity against *Plasmodium falciparum* using the standard membrane feeding assay. For two of the derivatives, BT37 and BT122, we observed a consistent dose–response relationship between concentration in the blood meal and oocyst intensity in the midgut. To explore their mechanism of action, we used the murine model *Plasmodium berghei* and found that both derivatives prevent ookinete maturation. Using fluorescence microscopy, we demonstrated that in the presence of each compound zygote vitality was severely affected, and those that did survive failed to elongate and mature into ookinetes. The observed phenotypes were similar to those described for mutants of specific kinases (NEK2/NEK4) and of inner membrane complex 1 (IMC1) proteins, which are all vital to the zygote-to-ookinete transition. We discuss the implications of our findings and our high-throughput screening

[*]**Corresponding Author:** Tel. +1-352-294-8448. rdinglasan@epi.ufl.edu.

[‖]Department of Entomology & Plant Pathology, Auburn University, Auburn, AL, United States

[⊥]Department of Biochemistry, Molecular Biology, Entomology and Plant Pathology, Mississippi State University, Mississippi State, MS, United States

[#]Emerging Pathogens Institute, Department of Infectious Diseases & Pathology, The University of Florida, Gainesville, FL, United States

[∇]Authors contributed equally

Supporting Information

The Supporting Information is available free of charge on the ACS Publications website at DOI: 10.1021/acschembio.6b00902.

Figure S1 and Table S1 (PDF)

The authors declare no competing financial interest.

approach to identifying next generation, transmission-blocking antimalarials based on the scaffolds of these (+)-usnic acid derivatives.

Graphical Abstract

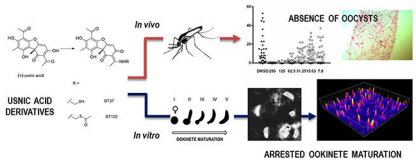

Despite substantial efforts to control malaria, more than 200 million cases and roughly 500 000 deaths per year are still attributed to the disease according to the most recent report from the World Health Organization.[1] *Plasmodium* parasites, the causative agent of the disease, have a complex life cycle that in the human host includes parasite development and asexual reproduction in the liver followed by cycles of similar processes in red blood cells (RBCs). The erythrocytic cycle produces a small fraction of parasites that differentiate into gametocytes, the only parasite stage capable of passing the infection from host to vector, mosquitoes in the genus *Anopheles*. Once in a mosquito gut, gametocytes egress from RBCs and rapidly differentiate into macro- and microgametes, which undergo sexual reproduction to produce zygotes. The zygotes develop into motile ookinetes, which invade the midgut epithelium to form oocysts in the basal lamina of the midgut wall. Oocysts are the sites where sporozoites develop, the only stage infectious to humans, which are delivered to new hosts through salivary secretions during biting.

In the human host, parasite development inside RBCs leads to red cell rupture and reinvasion of healthy RBCs. This erythrocytic cycle is responsible for stereotypical symptoms of malaria (fever, chills, and anemia) and is understandably why efforts to develop antimalarial drugs and vaccines have largely focused on blood-stage parasites. Emergence of resistance to the most commonly used antimalarial drugs has left malaria endemic countries relying primarily on artemisinin-based combination therapies (ACTs) to control the disease.[2] However, artemisinin resistance has emerged in *Plasmodium falciparum* populations in Southeast Asia, once again threatening malaria control in the region.[3] From a historical perspective, this is a common theme, as malaria parasites have repeatedly shown the ability to evolve resistance to frontline drugs.[4] To overcome this problem, discovery and development of new antimalarials that target multiple stages of the life cycle, including transmission-blocking (T-B) approaches, are sorely needed. Moreover, such a multipronged approach is particularly warranted given the ongoing debate on the merits of control versus a shift toward policies that favor regional elimination where feasible with the ultimate goal of global eradication.[5] Thus, from a strategic standpoint, drug development must focus on novel targets in erythrocytic stages that aim to cure malaria, as well as approaches that aim to prevent transmission. The latter may target either gametocytes, the link between human hosts and vectors, or the multistage process of parasite development inside the mosquito. Transmission blocking represents a relatively recent area of research that if successful will not only open new avenues to combat malaria but will make the argument for a policy shift toward elimination more compelling. To this end, it was recently shown that known

antimalarials and certain drugs with poor activity against the blood-stage parasites were successfully tested against mosquito stages and showed promise as T-B compounds.[6] Here, we take a similar approach by investigating a few derivatives of a natural product called (+)-usnic acid (UA), which is known to have weak antimalarial properties against multiple stages in the human host.[7,8] Our goal was 2-fold: first, to test whether these derivatives have activity against mosquito-stage parasites and, second, to investigate potential mechanisms of action for UA's antiparasitic properties.

UA is a yellow pigment produced as a secondary metabolite by lichens and classified chemically as a dibenzo-furandione.[7] The chemical is unique to lichens of the widely distributed genus *Usnea*, has been extensively studied, and is used in a range of therapeutic capacities, including wound healing, as an expectorant, a pain reliever, and as a preservative among others.[7,9–11] In a microbiological context, UA was found to have antimicrobial, antiviral, and antiprotozoal properties, as well as antiproliferative activity.[12] However, as a compound, UA has limited utility due to rapid metabolism, poor water solubility, lipophilic properties, and hepatotoxicity in mammals.[12,13] Nevertheless, it has shown great promise as an antiprotozoal. UA was effective against *Trichomonas vaginalis* with better inhibitory effects than metronidazole,[14] and previous studies with *Plasmodium* have demonstrated that UA has antimalarial activity against both blood and liver stages at micromolar concentrations.[8] Interestingly, UA was more effective against liver stages, as the IC_{50} was 20 times lower than the IC_{50} for blood stages, and when compared to primaquine, a liver schizonticidal drug, UA proved to be 4 times more effective.[8]

In an effort to improve UA antimalarial properties, a series of UA derivatives were synthesized by conjugating the compound to a variety of amine groups or amino acids. Biochemically, the goal of the conjugations was to increase UA solubility, minimize toxicity, and generate structural diversity off a common UA scaffold.[7] Bruno *et al*. tested effects of the derivatives against *P. falciparum* blood stages and found that some of the compounds showed antimalarial activity at lower micromolar concentrations.[7] Because of their activity against asexual stages in RBCs, as well as the activity of UA alone against liver stages, UA derivatives provide a promising starting point for developing new T-B compounds. To date, the molecular basis for antimalarial activity of UA and its derivatives is unknown, although *in vitro* studies with other organisms have demonstrated uncoupling of oxidative phosphorylation in mitochondria.[15] In *Plasmodium*, UA has been shown to inhibit vitamin E biosynthesis, but effects on other cellular processes in the parasite have not been ruled out.[16–18] Due to UA's lipophilic nature, it is recognized to be a membrane disruptor and in some cases may decrease lipid peroxidation while increasing the activity of enzymes involved in the antioxidative response.[17–19] Therefore, our approach here is to not only evaluate the efficacy of the derivatives during the mosquito stages but also to pinpoint developmental processes that may be affected. Our ultimate goal is to identify biochemical pathways in *Plasmodium* that have yet to be explored as drug targets.

RESULTS AND DISCUSSION

Usnic Acid Derivatives.

Six compounds were successfully synthesized by modification of UA (Figure 1a).[7,20] The chemical modification of the enolized β-diketone moiety into a stable enamine eliminated the portion responsible for membrane disruption. Of the six derivatives, four involved the addition of functional groups aimed at changing its chemical properties (e.g., reduced toxicity, increased solubility), while the remaining two linked UA to compounds with known antimalarial properties. Compound PS2 was synthesized by the addition of arginine to the UA molecule, compound PS7 by the addition of benzylamine, and compound BT37 by the addition of a sulfhydryl (SH) group. The latter was further esterified to give BT122, thus limiting the thiol reactivity. The antimalarial derivatives, compounds ME80 and PS4, were synthesized by the addition of GABA-artemisinin and quinoline to the UA backbone, respectively.

UA Derivatives Exhibit Transmission-Blocking Activity.

An initial screen of UA derivatives using the standard membrane feeding assay (SMFA) was performed with each compound at a high concentration (500 μg/mL) to identify promising derivatives for follow-up studies. In this assay, the compounds were added at the time of feeding, so there was no preincubation with gametocytes. Therefore, the duration of parasite exposure to each compound was limited to approximately 18–24 h, which spanned the time from mixing a compound with gametocytemic blood until the point of midgut invasion by the ookinete. Analysis of *Anopheles gambiae* midguts 8 days postfeeding revealed a dramatic reduction in *P. falciparum* oocysts relative to controls in five of the six compounds tested (95–100% inhibition of *P. falciparum* oocyst development; data not shown). A second set of experiments was performed at a lower concentration (250 μg/mL) with these five compounds. At this lower concentration, PS2 failed to inhibit oocyst formation and was therefore removed from our follow-up list. For compound ME80, percent inhibition fell below 95% and was also removed. The remaining four compounds (PS4, PS7, BT37, and BT122) demonstrated 99.3–100% inhibition of *P. falciparum* oocyst development in replicate experiments (Figure 1b and c). For the remaining experiments presented below, we focus on BT37 and BT122 due to their potential for targeting novel pathways for antimalarial activity, as they may be related to the same mechanism of action. Both PS4 and PS7 will be followed further in subsequent studies.

It should be noted that results from the highest concentrations, particularly our initial screen, may reflect cytotoxicity of the compounds rather than a specific effect on *Plasmodium*. Previously reported data from a toxicity study for BT37 using HaCaT keratinocytes (compound 8 in Table 1, ref 20), found that following a 24-h exposure the LC_{50} was 155 μg/mL (95% CI = 116–207 μg/mL). Out of concern, we performed additional toxicity assays for both BT37 and BT122 using three cell lines, L6 (rat myoblast), RAW 264.7 (mouse monocyte/macrophage), and HepG2 (human hepatocyte). Following exposure to compounds for 24 and 48 h, cell viability for each line was assayed using alamarBlue, and lethal concentration 50 (LC_{50}) and lethal concentration 05 (LC_{05}) values were estimated by nonlinear regression, which respectively refer to the concentrations at which 50% and 5% of

the cells were inviable following exposure to a compound for a given length of time. The assays revealed consistent LC_{50} and LC_{05} values for all three lines at both time points. At 24 h, the time point most relevant for SMFAs and our subsequent experiments, the LC_{50} and LC_{05} for BT37 ranged respectively from lows of 504.9 μg/mL (95% CI = 466−553 μg/mL) and 55.0 μg/mL (95% CI = 40−75 μg/mL) for L6 to highs of 638.2 μg/mL (95% CI = 584−712 μg/mL) and 107.1 μg/mL (95% CI = 75−151 μg/mL) for RAW 264.7 (Table S1). For BT122, the LC_{50} and LC_{05} estimates were generally higher, ranging from lows of 603.1 μg/mL (95% CI = 539−693 μg/mL) and 64.7 μg/mL (95% CI = 75−151 μg/mL) for L6 to highs of 731.2 μg/mL (95% CI = 618−918 μg/mL) for RAW 264.7 and 86.3 (95% CI = 54−136 μg/mL) for HepG2 (Table S1). Given that BT122 is an esterified form of BT37 that was synthesized with the goal of masking BT37's highly reactive thiol group, this somewhat lower toxicity level was expected. After exposure to the compounds for 48 h (Table S1), cell viability was substantially lower, and although this time point has no bearing on parasite development within the midgut, we include the data in Table S1 for its potential relevance to safety in the human host.

Dose-Ranging Experiments for BT37 and BT122.

To further analyze the efficacy of BT37 and BT122 as T-B compounds, we performed dose ranging experiments to determine if there was a dose–response effect on oocyst development for each and, if so, estimate their half maximal inhibitory concentrations (IC_{50}). These experiments followed the same protocol as the above SMFAs with the addition of a membrane feeder for each concentration per derivative of a 2-fold dilution series beginning at 250 μg/mL. At the highest two concentrations, both derivatives showed 100% inhibition of oocyst development in replicated experiments (Figure 2). At lower concentrations, the percent inhibition for BT37 ranged from 84.8% at 62.5 μg/mL to 0% at 7.8 μg/mL and for BT122 from 92% inhibition at 62.5 μg/mL to 0% inhibition at 7.8 μg/mL (Figure 2). The IC_{50} of each compound was estimated by logistic regression from the dose–response data and ranged from 37.2 to 55.5 μg/mL for BT37 (97–142 μM) and 14.2–101.6 μg/mL (35–234 μM) for BT122 (Figure S1).

Assessment of UA-Derivative Impact on Microgametogenesis and Ookinete Development in *P. berghei* and *P. falciparum*.

To explore effects on transmissible (human-to-mosquito) parasite stages found in the mosquito blood meal (gametocytes) and on those that develop in the mosquito midgut within the first 24 h post feeding (gametes, zygotes, ookinetes), we performed follow-up experiments with *P. berghei* and *P. falciparum* using BT37 and BT122. To assess whether either compound affects the process of microgametogenesis, gametocytes from *P. berghei*-infected mice and *P. falciparum* gametocyte cultures were exposed separately to BT37 and BT122 and then analyzed by microscopy for exflagellating microgametes. In DMSO-only negative controls, exflagellation was higher for *P. berghei* than for *P. falciparum*, but for each parasite species the number of exflagellation centers for BT37 and BT122 were similar to that of the negative controls. Only the positive control (aphidicolin) showed reduced exflagellation, and when the data were analyzed by negative binomial regression, there was no effect of treatment when the positive controls were removed from the analysis (*P. berghei:* $z = 0.28$, $p = 0.777$; *P. falciparum:* $z = 0.50$, $p = 0.614$; Figure 3). Therefore, the data

indicated no impact of either BT37 or BT122 on microgametogenesis when gametocytes were exposed to each compound for a short period of time (approximately 15 min). Unlike microgametes, macrogametes are difficult to distinguish from zygotes, and we were unable to determine if there was an effect on this stage or the process of fertilization. We acknowledge that the compounds may act in this portion of the life cycle.

To investigate ookinete development, *P. berghei* ookinete cultures were treated with 250 μg/mL of BT37 or BT122 upon culture initiation. At 24 h post-treatment, immunofluorescence assays (IFAs) showed fully developed ookinetes in the DMSO control groups, but mature ookinetes could not be detected in the UA-derivative groups (Figure 4a). Instead of mature ookinetes or partially developed retorts, small round cells expressing Pbs21 protein were stained in the IFAs and were much more commonly found in the BT37 and BT122 cultures. Since Pbs21 translation is repressed in gametocytes, this staining pattern in the treated cultures suggests that the round cells were either (i) unfertilized macrogametes, (ii) zygotes that arrested soon after fertilization, or (iii) zygotes that began the ookinete developmental program but failed to elongate like normal ookinetes. Similar to these findings for *P. berghei*, *P. falciparum* ookinetes failed to develop inside the mosquito when gametocytes were cofed with the UA derivative BT122 in a blood meal. Ookinete development for this species was investigated using an *ex vivo* approach due to difficulty in culturing large numbers of ookinetes unlike *P. berghei*. Staining patterns for Pfs28 (ortholog of Pbs21 in *P. falciparum*) on these blood-meal-derived parasites showed Pfs28-positive round cells for the treated group and elongating retorts in the DMSO control group (Figure 4b). These results support the SMFA data and provide insight into the reduction of oocyst intensity in the BT37 and BT122 groups.

Recognizing the possibility of sporozoite development in the few oocysts seen in the treated midguts, we fed mosquitoes as above with gametocytemic blood containing 125 μg/mL of BT37 or DMSO (as control) and allowed the infection to progress until day 18. All surviving mosquitoes were ground individually, and homogenates were used in a sporozoite ELISA with a peroxidase-conjugated monoclonal antibody to circumsporozoite protein for detection.[21] We found that all mosquitoes tested positive for sporozoites in the DMSO control group, but sporozoites were detected in only 3 of 34 mosquitoes (8.8%) in the BT37 treatment group (data not shown), suggesting that most oocysts that did develop failed to produce sporozoites (note that oocyst prevalence for the 125 μg/mL treatment groups in Figure 2 was 29% for BT37 in mosquitoes dissected at day 8).

Usnic Acid Derivatives Impact *P. berghei* Zygotes and Impair Ookinete Development in a Dose-Dependent Manner.

To explore further the influence of BT37 and BT122 on ookinete development, a recently described, high-throughput assay that uses a genetically modified strain of *P. berghei* that expresses GFP driven by the CTRP promoter was employed.[22] Briefly, ookinete cultures were started as above, but each UA derivative was added at culture initiation in a 1:1.4 dilution series starting at 125 μg/mL (highest concentration) along with a carrier-only (DMSO) negative control and a positive control (cycloheximide) that completely inhibits ookinete development. Each set of treatments and controls was replicated across four 96-

well plates, and all wells were imaged with an epifluorescence microscope after 24 h. The extent of ookinete development was analyzed by measuring fluorescence intensity from images and comparing the number of fluorescent parasites in two shape classes, round cells and retorts/ookinetes. These cell types are easily distinguished by eye, and even though retorts (gourd-shaped) are distinct from mature ookinetes (banana-shaped), we chose to be conservative and group them together since the elongation process, which reflects progression approximately 5–6 h down the pathway toward ookinete maturation,[23] had clearly begun in the retorts. Representative images from these assays and the mean number of parasites in each shape class expressing GFP are presented in Figures 5 and 6. As observed in the IFAs using anti-Pbs21, *P. berghei* ookinete development was inhibited by the addition of BT37 and BT122 to the *in vitro* cultures. Among treatment groups, the presence of round parasites was predominant at the two highest concentrations tested for each compound, consistent with SMFA data described above. Because CTRP expression begins ~7–10 h post fertilization[22,24] and because neither compound affects exflagellation (Figure 3), we believe that these round cells are zygotes/ookinetes that failed to mature, which provides a rough approximation of the time window during which the compounds likely acted. Any round cells producing GFP must have been at least several hours post fertilization, a point at which elongation has typically already begun.[23] The fact that these cells expressed CTRP-GFP yet were still round suggests that either elongation was inhibited or the zygotes that survived to the point of CTRP expression were severely altered. Either way, it appears that for most zygotes normal cellular processes continued for only a short time after fertilization before developing zygotes/ookinetes arrested. This is most apparent by comparisons of the total number of fluorescent cells (i.e., ookinetes plus round cells) for UA-derivative treatments with the number of fluorescent cells in the control group (Figures 6b,c). For BT37, this number was reduced by 95.1% and 86.5% in the 125 μg/mL and 63.8 μg/mL treatments, respectively, but showed no reduction in lower concentrations. For BT122, the results were similar, but the effect was more pronounced for the highest concentration treatments, as the total fluorescent cells relative to controls was reduced by more than 99% at 125 μg/mL and 63.8 μg/mL. Thus, the effect of BT37 and BT122 is likely most pronounced on zygotes, although an impact on macrogametes cannot be ruled out.

With this approach, we were able to follow up on initial observations of reduced and abnormal ookinete development in IFAs and show that zygote death and failed ookinete elongation was a consistent outcome following treatment with BT37 and BT122, therefore pinpointing the stages of the parasite in which these compounds acted. Although we lacked the same assay capability with *P. falciparum*, parasite morphology in blood meals dissected from mosquitoes 22–24 h post blood feeding suggest that both compounds acted similarly against this agent of human malaria. These results further suggest that the UA derivatives targeted the same pathway(s) in both species.

Potential Mechanisms for UA-Derivative Impact on Zygotes and Ookinete Development.

As reported above, UA derivatives likely disrupt one or more cellular processes that occur after gametogenesis but before expression of CTRP ~ 6–7 h post fertilization. Once fertilization occurs, the diploid zygote undergoes karyogamy followed by meiosis without cell division, resulting in a tetraploid early ookinete that has yet to elongate into its

characteristic shape.[25] Studies of *Plasmodium* protein kinases during the zygote-to-ookinete transition found that mutations in two of these enzymes, NEK2 and NEK4, cause dysregulated DNA replication during meiosis in the zygote and the absence of mature ookinetes.[26–28] Although we have no reason to believe that the UA derivatives interact with these kinases or interfere with phosphorylation, the fact that NEK2/NEK4 mutants arrest at approximately the same time as most BT37/BT122-treated zygotes points to a cellular process that UA derivatives may impair. Alternatively, we cannot rule out that the zygote is simply more sensitive to toxicity than gametocytes or gametes.

For the BT37/BT122-treated ookinetes that express CTRP but fail to elongate, the observed phenotypes are similar to those in a recent description of inner membrane complex 1 (IMC1) protein mutants.[29] The inner membrane complex (IMC) is composed of flattened vesicles called alveoli, which lie beneath the plasma membrane and are supported by a network of filamentous proteins called the subpellicular network, as well as by interactions with the cytoskeleton.[30,31] The IMC consists of lipids and a number of associated proteins, is dynamic throughout the *Plasmodium* life cycle, and is known to have at least three important roles. It is involved in cell morphology and stability, is used as a scaffold during the formation of daughter cells, and is involved in motility and the process of cell invasion.[30,31] Regulation of IMC and its supporting subpellicular microtubule network (SPN) is critical to maturation of the gametocyte and stages of *P. falciparum* specific to the mosquito. Gametocyte elongation and rigidity is mediated by the IMC and SPN and allows the parasite to sequester in the bone marrow.[30,32] Loss of this rigidity results in the release of the mature, stage V gametocyte into the peripheral blood, enabling transmission to blood feeding mosquitoes. It has been suggested that morphological changes during ookinete development are also driven by formation of the IMC and the SPN.[29,31] In accordance with this, *P. berghei* ookinetes in which IMC1b or IMC1h were knocked out failed to develop normally.[29,33] These ookinetes partially elongated but formed a bottleneck between the zygote body and the ookinete protrusion.

At least 17 structural proteins have been linked to the *Plasmodium* IMC,[26] including seven alveolins and four six-transmembrane proteins, and IMC proteins have been shown to form part of the parasite's glideosome.[34,35] However, it remains unclear if usnic acid derivatives directly target IMC proteins, lipid components of the IMC, or enzymes involved in IMC regulation. Because UA is known to be lipophilic,[36] one intriguing hypothesis is that BT37 and BT122, which should no longer have membrane insertion capabilities due to the described modifications to the UA scaffold, disrupt the IMC alveoli through different interactions with lipid moieties. Although little is known about their lipid composition in *Plasmodium*, studies in *Toxoplasma gondii* indicate the presence of both cholesterol[37,38] and phosphoinositides.[39] While the former anchors the glideosome to the IMC through interactions with GAP50,[38] the latter may carry out a variety of functions, including cell signaling, regulation of membrane traffic, and interactions with the cytoskeleton.[40] Alternatively, usnic acid derivatives may target proteins involved in the fatty acid biosynthesis (FAS-II) pathway, as has been postulated in the study of inhibitory activity of lichen-derived metabolites against *Plasmodium* liver stages.[8] We hypothesize that BT37 and BT122 inhibition of FAS-II may indirectly interfere with palmitoylation-mediated protein trafficking to the IMC and SPN, as has been described for *Toxoplasma*[41] and more recently

in *Plasmodium*.[42] To our knowledge, no direct link exists between FAS-II inhibition and morphological phenotypes for the extracellular, mosquito stages of *Plasmodium*.[43] However, the palmitoyl-S-acyl transferase $DHHC_2$ was recently shown to be essential for ookinete morphogenesis[44] as inhibition of palmitoylation yielded round zygotes that had undergone meiosis but failed to elongate into ookinetes. Presumably, inhibition of palmitate synthesis would yield a similar phenotype. Thus, we cannot rule out the possibility that the mode of action of UA derivatives in ookinete development is related to its potential pleiotropic inhibition of IMC and SPN protein function, alveoli structure, and fatty acid synthesis.

Natural Product Screens for Next Generation Anti-malarials.

Antimalarials may have multiple modes of action, and high throughput screens (HTS) of libraries can easily miss potential candidates, especially if the assay is limited to a parasiticidal read-out. Similar to BT37 and BT122, a number of compounds derived from natural products have been found to impact sporogonic stages of *Plasmodium*. The plant-derived compounds azadirachtin and colchine, for example, limit ookinete production and have been hypothesized to inhibit tubulin polymerization,[45,46] a process that, as outlined above, is critical to the formation of the subpellicular network during ookinete maturation. Additionally, azadirachtin and some of its derivatives block microgametogenesis,[47] demonstrating the potential of natural-product derivatives to target multiple sporogonic stages.

The repeated evolution of drug resistance in *Plasmodium* spp. indicates the need to get ahead of the parasite in the “arms race” and to target both the asexual and sexual stages. To enable discovery and optimization of transmission-blocking drugs, we argue that approaches such as the one employed here are essential. The ookinete development assay (ODA) using high-content imaging microscopy represents a powerful approach for evaluating the effect of compounds on parasite development that would otherwise fall-out of a parasite-killing screen, and such a strategy has recently proven successful in HTS assays for *P. falciparum*.[48] Moreover, because the ODA readout is the mature ookinete, this approach will identify compounds that act on any of the processes or stages between gametogenesis and ookinete maturation. Through the ODA and follow-up studies, we have confirmed that usnic acid derivatives impact sporogonic development, likely acting on processes vital to the zygote-to-ookinete transition. Given the mirrored effect of these compounds for both *P. berghei* and *P. falciparum*, we anticipate the HTS of additional usnic acid derivative scaffolds that can ultimately lead to new compounds following medicinal chemistry optimization. These derivatives can be further modified to develop new chemical biology probes to identify the exact biological target(s) in *Plasmodium*. Importantly, the same strategy can be applied to the HTS assay of other existing natural product metabolites and small molecules that have escaped consideration as potential transmission-blocking compounds.

METHODS

Synthesis of Usnic Acid Derivatives.

Compounds ME80, PS2, PS4, PS7, and BT37 were synthesized as previously described.[7,20] Briefly, commercially available (+)-usnic acid was refluxed in EtOH, $EtOH/H_2O$, or

EtOH/THF and treated with the appropriate amine or amino acid until disappearance of the starting material. The reaction mixture was concentrated *in vacuo*, and the crude material was purified by crystallization. To synthesize BT122, acetic anhydride (36 μL, 0.37 mmol) was added to a solution of BT37 (150 mg, 0.37 mmol) in pyridine (92 μL) and dichloromethane (1.5 mL) under He, and the reaction mixture was stirred at RT for 2 h. Solvent was evaporated until dryness, and the crude product was purified by flash-chromatography (*n*-hexane/ethyl acetate 7:3) to give 156 mg (0.35 mmol, 95%) of yellow solid (R*f* 0.25, eluent: *n*-hexane/ethyl acetate 7:3). The product was characterized through ^{1}H and ^{13}C NMR and ESIMS spectroscopy. ^{1}H NMR 400 MHz ($CDCl_3$): δ 1.72 (s, 3H, CH_3-13), 2.11 (s, 3H, CH_3-16), 2.42 (s, 3H, $\underline{CH_3}CO$), 2.69 (s, 6H, CH_3-15 and CH_3-18), 3.17 (t, J = 6.8 Hz, 2H, CH_2-2′), 3.68–3.73 (m, 2H, CH_2-1′), 5.81 (s, 1H, CH-4), 11.86 (s, 1H, OH-10), 13.37 (s, 1H, OH-8), 13.50 (br s, 1H, NH). ^{13}C NMR 100 MHz ($CDCl_3$): δ 6.98 (C-16), 17.76 (C-15), 27.71 (C-2′), 30.15 ($\underline{CH_3}CO$), 30.76 (C-18), 31.45 (C-13), 42.68 (C-1′), 56.77 (C-12), 100.89 (C-2 + C-7), 101.97 (C-4), 104.52 (C-11), 107.56 (C-9), 155.37 (C-6), 157.74 (C-10), 163.03 (C-8), 173.69 (C-5), 174.86 (C-14), 194.28 (C-3 and $CH_3\underline{CO}$), 197.98 (C-1), 201.17 (C-17). MS (ESI), negative, *m/z* 444.1 $[M - H]^-$; calculated for $C_{22}H_{23}NO_7S$: 445.1.

Animal Welfare.

All experimental studies using mice were performed in accordance with Johns Hopkins University (JHU) ACUC (Animal Welfare Assurance #A3272–1) regulations and the EU regulations “EU Directive 86/609/EEC” and within the regulations of the United Kingdom Animals (Scientific Procedures) Act 1986. The Animal Protocol (#MO12H232) used for these studies was reviewed and approved by the JHU ACUC and are in compliance with the United States Animal Welfare Act regulations and Public Health Service (PHS) Policy. No human subject research was performed during this study.

Transmission-Blocking Assays.

Transmission-blocking assays were performed using the human malaria parasite *P. falciparum* and *Anopheles gambiae* mosquitoes.[49,50] For each experiment, the age of the gametocyte culture (16–17 days), the age of mosquitoes (4–6 days), the blood-meal gametocytemia (0.2%), and hematocrit (45%) were kept consistent. For each experimental treatment, the usnic acid derivative was diluted in DMSO to a stock concentration of 33.3 mg mL^{-1} and diluted to experimental concentrations with human blood. For dilution series, concentrations of DMSO were adjusted for each dilution as necessary to maintain a constant DMSO concentration across dilutions. For each treatment, mosquitoes (n = 40–50) were allowed to feed to repletion. All mosquitoes were knocked down on ice in a 4 °C room, and unfed mosquitoes were then removed from cups. Following blood feeding, mosquitoes were maintained on sucrose and water for 8 days at 26 °C and 80% relative humidity. On day 8 post blood feeding, midguts were dissected from all surviving mosquitoes and stained with 0.1% mercurochrome for 20 min. The oocyst number for each midgut was determined by microscopy, and at least two independent experiments were performed for the dilution series for each compound.

Toxicity Assays.

The L6 rat myoblast cell line (a generous gift from G. Wong, Johns Hopkins School of Medicine, Baltimore, MD) was propagated in low-glucose DMEM supplemented with 10% fetal bovine serum albumin (FBS) and 1% penicillin–streptomycin (P–S). The RAW 264.7 mouse leukemic monocyte-macrophage cell line (American Type Culture Collection TIB-71) and HepG2 hepatocellular carcinoma cell line (a kind gift from P. Sinnis) were cultured in DMEM supplemented with 10% FBS and 1% P–S. All cell lines were maintained at 37 °C in a 5% CO_2 chamber. Forty-eight h prior to drug addition, L6, RAW 264.7, and HepG2 cells were seeded in 96-well plates at a density of 5000 cells/well. Cells were incubated with 2-fold serial dilutions of BT-37 or BT-122 ranging from 500 to 0.1 μg/mL for 24 or 48 h. Control wells contained media with the highest equivalent concentration of DMSO. At 24 or 48 h post drug addition, 10 μL of alamarBlue reagent (ThermoFisher Scientific) was added to the wells, and plates were further incubated at 37 °C for 4 h. Three independent biological replicate experiments were performed with three technical replicates per compound dose. The plates were read using a Spectramax M2 microplate reader (Molecular Devices, Sunnyvale, CA) with excitation/emission wavelengths set at 544/590 nm. LC_{50} and LC_{05} values were calculated by nonlinear regression from sigmoidal dose–response curves generated using GraphPad Prism software (v. 7.0).

Microgametogenesis Assays.

Assays were performed to test the effect of UA derivatives on microgametogenesis for both *P. berghei* and *P. falciparum*. For the former, female Swiss Webster mice were phenylhydrazine treated (i.p.) 3 days prior to injection with blood from a donor mouse (i.v., ~ 10% parasitemia) infected with *P. berghei* ANKA strain. The day after injection, mice were treated with 200 μL of a 1 mg mL^{-1} pyrimethamine (PYR) solution (i.p.) and used in microgametogenesis assays the following day. For each replicate, 1.5 μL of blood was taken from tail snip and mixed with DMSO, aphidicolin (125 nM), BT37 (250 μg/mL), or BT122 (250 μg/mL) in 7.5 μL of ookinete media and 1 μL of heparin working stock (1 ng/μL). The mixture was incubated for 10 min, spotted on a glass slide, and covered with a coverslip (18 mm × 18 mm). The number of exflagellation centers was then counted for five fields. For each treatment group, this was replicated three times (technical replicates) across three mice (biological replicates). For *P. falciparum* (NF54), cultured gametocytes (day 17) were used in a similar assay in which 20 μL of settled culture (2% gametocytemia) were mixed with DMSO, aphidicolin, BT37, or BT122 at the same concentrations as above. After a 10 min incubation, 4 μL was spotted on a glass slide, covered with a coverslip, and scored for exflagellation centers in five fields per replicate. The assay was replicated three times (technical replicates) from three separate cultures (biological replicates).

Ookinete Cultures.

Female Swiss Webster mice were phenylhydrazine treated (i.p.) 3 days prior to infection with *P. berghei* ANKA strain parasites from a donor mouse with at least 10% parasitemia. One day after infection, the mice were treated with 200 μL of a 1 mg mL^{-1} pyrimethamine (PYR) solution (i.p.). One day after PYR treatment, all infected mice were tested for

exflagellation. Mice with at least 10 exflagellation centers per field (40× objective) were sacrificed, the blood collected by cardiac puncture and used to initiate ookinete cultures. Infected blood was diluted 1:20 with complete ookinete medium[51] and incubated at 19 °C for 24 h with slow shaking. Parasites were harvested by centrifugation and development was assessed by immunofluorescence assay as described below.

Immunostaining of *P. berghei* and *P. falciparum* Ookinetes.

P. berghei parasites (ANKA strain) from ookinete cultures were fixed with 4% paraformaldehyde and prepared for fluorescence microscopy by washing three times with PBS. After washing, samples were blocked with 3% BSA in PBS for 1 h at RT. The samples were then incubated with mouse anti-Pbs21 (1:1000) for 1 h at RT. Cells were washed with PBS as before and detected with Alexa Fluor(R) 594 goat antimouse IgG (H+L), highly cross-adsorbed (Molecular Probes, 1:1000) for 1 h at RT. Following incubation, the cells were washed three times with PBS, resuspended in PBS, spotted on slides, and allowed to air-dry. Samples were mounted using Slow Fade Gold antifade reagent with DAPI (Molecular Probes) and examined using a Nikon Upright E800 microscope with SPOT software. Blood meals from mosquitoes fed with *P. falciparum* gametocytes and one of the UA derivatives or DMSO alone were removed from midguts dissected 20–24 h postfeeding. Dissected blood meals were pooled from 25 mosquitoes per treatment, washed with PBS, and fixed with 4% paraformaldehyde for 30 min before preparing for fluorescence microscopy as described above using antibodies against Pfs28, a *P. falciparum* zygote, and ookinete surface marker homologous to Pbs21.

Fluorescent Ookinete Development Assay.

This assay was performed in 96-well plates as described by Delves *et al.*[22] using the *P. berghei* strain PbCTRPp.GFP, which has a GFP expression cassette under the control of the CTRP promoter.[52] Briefly, UA derivatives (BT37 and BT122) were tested in ookinete cultures starting at a concentration of 125 μg/mL in DMSO and serially diluted 1:1.4 to final concentrations in 0.75% DMSO. The same percentage of DMSO was used as a negative control, and 20 μM cycloheximide, a known inhibitor of exflagellation that prevents fertilization and subsequent ookinete development, was used as a positive control to determine background fluorescence for each plate. Experiments were performed in quadruplicate independently, with each replicate using parasite-infected blood from a different mouse. Upon exsanguination *via* cardiac puncture, infected blood was mixed 1:20 with ookinete medium containing FBS (20%), dispensed into test plates using a Multidrop Combi automated dispenser (Thermo-Scientific), and gently mixed with test or control compounds. Plates were maintained in the dark at 19 °C for approximately 22 h, after which GFP-positive cells were imaged by automated fluorescence microscopy as described.[53] For each well, the numbers of ookinetes and round cells were counted using a size and shape algorithm in ImageJ v.1.49i (freely available at http://rsb.info.nih.gov/ij/). Images were prepared for counts manually by adjusting the fluorescence intensity to reduce background fluorescence (based on controls for each plate) and then setting a detection threshold. Fluorescing cells with signal intensities above the threshold were converted to binary black and white images and were then counted based on size and shape parameters. These parameters were determined empirically using the “Analyze Particles” option from the

"Analyze" dropdown menu, and the size range used for both cell types was set to 16–300. To distinguish shape, the parameter called "circularity" was set to 0–0.8 for ookinetes and 0.81–1.0 for round cells. For a subset of the images, fluorescing ookinetes and round cells were counted manually to test the automated system and assess bias or systematic error introduced by the process.

Statistical Methods.

To determine significance between treatment and control groups in the membrane feeding assays, the nonparametric Kruskal–Wallis test was used due to the non-normal distributions typical of oocyst counts. The test was performed comparing the distribution of oocyst counts per midgut among all groups, followed by Dunn's multiple comparisons test for each pairwise comparison between a treatment group and the DMSO control. To estimate the half maximal inhibitory concentration (IC_{50}) for oocyst development, percent inhibition was first calculated from SMFA data from the dose–response experiments as $((\text{median}_{\text{control}} - \text{median}_{\text{treatment}})/\text{median}_{\text{control}}) \times 100$. For each compound, the concentration was log transformed, and the following nonlinear model was applied to each replicate in GraphPad Prism (v. 7.0): $Y = \text{Bottom} + (\text{Top} - \text{Bottom})/(1 + 10\text{^}((X - \text{Log } IC_{50})))$, where Top and Bottom refer to plateaus in units of the Y axis. To determine if UA derivatives influenced microgametogenesis, the number of exflagellation centers per field was analyzed by negative binomial regression with treatment and mouse or culture as the main effects. To compare similarity of manual and automated counts of ookinetes and round cells, two approaches were used. First, proportions of round cells (note that the proportions of ookinetes are simply 1 minus those of round cells) were plotted against concentrations of BT122 on a log scale for both count methods. Similar to the IC_{50} calculations, four-parameter logistic curves were fit to each data set in GraphPad Prism (v. 7.0) using the nonlinear curve-fitting function. Parameter estimates and goodness of fit were then used to assess similarity of the two methods. Second, proportions of round cells from manual and automated counts of the same wells across three replicates (15 wells total) were plotted against one another. The Spearman nonparametric test for correlation was used to calculate a correlation coefficient (Spearman r) and estimate the probability that the observed coefficient was due to chance. Finally, to analyze data from the fluorescent ookinete development assay, means and standard errors for each concentration of BT37 and BT122 were calculated from counts of four replicates per concentration. Mean ookinete number was compared among treatments using one-way ANOVA, followed by Dunnett's test to compare each treatment mean with that of the control (DMSO only).

Supplementary Material

Refer to Web version on PubMed Central for supplementary material.

ACKNOWLEDGMENTS

This work was supported by R01AI082587 from the NIAID, National Institutes of Health (R.R.D.). The authors thank Dr. D. Monti for helpful discussions.

REFERENCES

(1). World Health Organization. (2015) World Malaria Report 2015, World Health Organization, Geneva, Switzerland Available: http://www.who.int/malaria/publications/world_malaria_report_2014/en/.

(2). World Health Organization. (2015) Guidelines for the Treatment of Malaria, 3rd ed., World Health Organization, Geneva, Switzerland Available: http://www.who.int/malaria/publications/atoz/9789241549127/en/.

(3). Dondorp AM, Nosten F, Yi P, Das D, Phyo AP, Tarning J, Lwin KM, Ariey F, Hanpithakpong W, Lee SJ, Ringwald P, Silamut K, Imwong M, Chotivanich K, Lim P, Herdman T, An SS, Yeung S, Singhasivanon P, Day NP, Lindegardh N, Socheat D, and White NJ (2009) Artemisinin resistance in Plasmodium falciparum malaria. N. Engl. J. Med 361, 455–467. [PubMed: 19641202]

(4). Plowe CV (2009) The evolution of drug-resistant malaria. Trans. R. Soc. Trop. Med. Hyg 103 (S1), S11–S14. [PubMed: 19084883]

(5). Alonso PL, Brown G, Arevalo-Herrera M, Binka F, Chitnis C, Collins F, Doumbo OK, Greenwood B, Hall BF, Levine MM, Mendis K, Newman RD, Plowe CV, Rodriguez MH, Sinden R, Slutsker L, and Tanner M (2011) A research agenda to underpin malaria eradication. PLoS Med 8 (1), e1000406. [PubMed: 21311579]

(6). Delves M, Plouffe D, Scheurer C, Meister S, Wittlin S, Sinden RE, Winzeler EA, and Leroy D (2012) The activities of current antimalarial drugs on the life cycle stages of Plasmodium: A comparative study with human and rodent parasites. PLoS Med 9 (2), e1001169. [PubMed: 22363211]

(7). Bruno M, Trucchi B, Monti D, Romeo S, Kaiser M, and Verotta L (2013) Synthesis of a potent antimalarial agent through natural products conjugation. ChemMedChem 8 (2), 221–225. [PubMed: 23307699]

(8). Lauinger IL, Vivas L, Perozzo R, Stairiker C, Tarun A, Zloh M, Zhang X, Xu H, Tonge PJ, Franzblau SG, Pham D-H, Esguerra CV, Crawford AD, Maes L, and Tasdemir D (2013) Potential of lichen secondary metabolites against Plasmodium liver stage parasites with FAS-II as the potential target. J. Nat. Prod 76 (6), 1064–1070. [PubMed: 23806111]

(9). Okuyama E, Umeyama K, Yamazaki M, Kinoshita Y, and Yamamoto Y (1995) Usnic acid and diffractaic acid as analgesic and antipyretic components of Usnea diffracta. Planta Med 61 (2), 113–115. [PubMed: 7753915]

(10). Vartia KO (1973) Antibiotics in lichens, in The Lichens (Ahmadjian V, and Hale ME, Eds.), pp 547–561, Academic Press, New York.

(11). Shibata S, Ukita T, Tamura T, and Miura Y (1948) Relation between chemical constitutions and antibacterial effects of usnic acid and its derivatives. Jpn. Med. J 1, 152–155.

(12). Ingólfsdóttir K (2002) Usnic Acid. Phytochemistry 61 (7), 729–736. [PubMed: 12453567]

(13). Frankos VH (2005) N.T.P. Nomination for Usnic Acid and Usnea Barbata, U.S. National Toxicology Program, Research Triangle Park, NC Available: http://ntp.niehs.nih.gov/ntp/htdocs/chem_background/exsumpdf/usnicacid_508.pdf.

(14). Guo L, Shi Q, Fang J-L, Mei N, Ali AA, Lewis SM, Leakey JA, and Frankos VH (2008) Review of usnic acid and Usnea barbata toxicity. J. Environ. Sci. Health. Part C: Environ. Carcinog. Ecotoxicol. Rev 26, 317–338.

(15). Han D, Matsumaru K, Rettori D, and Kaplowitz N (2004) Usnic acid-induced necrosis of cultured mouse hepatocytes: inhibition of mitochondrial function and oxidative stress. Biochem. Pharmacol 67, 439–451. [PubMed: 15037196]

(16). Verotta L, Appendino G, Bombardelli E, and Brun R (2007) In vitro antimalarial activity of hyperforin, a prenylated acylphloroglucinol: a structure-activity study. Bioorg. Med. Chem. Lett 17, 1544–1548. [PubMed: 17234416]

(17). Sussmann RAC, Angeli CB, Peres VJ, Kimura EA, and Katzin AM (2011) Intraerythrocytic stages of Plasmodium falciparum biosynthesize vitamin E. FEBS Lett 585 (24), 3985–3991. [PubMed: 22085796]

(18). Van der Meer J-Y, and Hirsch AKH (2012) The isoprenoid-precursor dependence of Plasmodium spp. Nat. Prod. Rep 29 (7), 721–728. [PubMed: 22555616]

(19). Kohlhardt-Floehr C, Boehm F, Troppens S, Lademann J, and Truscott TG (2010) Prooxidant and antioxidant behavior of usnic acid from lichens under UVB-light irradiation–studies on human cells. J. Photochem. Photobiol., B 101 (1), 97–102. [PubMed: 20656501]

(20). Bruno M, Trucchi B, Burlando B, Ranzato E, Martinotti S, Akkol EK, Süntar I, Keles H, and Verotta L (2013) +)-Usnic acid enamines with remarkable cicatrizing properties. Bioorg. Med. Chem 21 (7), 1834–1843. [PubMed: 23434134]

(21). Burkot TR, Zavala F, Gwadz RW, Collins FH, Nussenzweig RS, and Roberts DR (1984) Identification of malaria-infected mosquitoes by a double antibody enzyme-linked immunosorbent assay. Am. J. Trop. Med. Hyg 33 (2), 227–231. [PubMed: 6370003]

(22). Delves MJ, Ramakrishnan C, Blagborough AM, Leroy D, Wells TNC, and Sinden RE (2012) A high-throughput assay for the identification of malarial transmission-blocking drugs and vaccines. Int. J. Parasitol 42, 999–1006. [PubMed: 23023046]

(23). Janse CJ, Mons B, Rouwenhorst RJ, Van der Klooster PF, Overdulve JP, and Van der Kaay HJ (1985) In vitro formation of ookinetes and functional maturity of Plasmodium berghei gametocytes. Parasitology 91 (1), 19–29. [PubMed: 2863802]

(24). Yuda M, Sawai T, and Chinzei Y (1999) Structure and expression of an adhesive protein-like molecule of mosquito invasive-stage malarial parasite. J. Exp. Med 189 (12), 1947–52. [PubMed: 10377190]

(25). Guttery DS, Roques M, Holder AA, and Tewari R (2015) Commit and Transmit: Molecular players in Plasmodium sexual development and zygote differentiation. Trends Parasitol 31 (12), 676–685. [PubMed: 26440790]

(26). Reininger L, Billker O, Mukhopadhyay A, Fennell C, Dorin-Semblat D, Doerig C, Harmse L, Ranford-Cartwright L, Packer J, Doerig C, Tewari R, and Goldring D (2005) A NIMA-related protein kinase is essential for completion of the sexual cycle of malaria parasites. J. Biol. Chem 280 (36), 31957–31964. [PubMed: 15970588]

(27). Reininger L, Tewari R, Fennell C, Holland Z, Goldring D, Ranford-Cartwright L, Billker O, and Doerig C (2009) An essential role for the Plasmodium Nek-2 Nima-related protein kinase in the sexual development of malaria parasites. J. Biol. Chem 284 (31), 20858–20868. [PubMed: 19491095]

(28). Tewari R, Straschil U, Bateman A, Böhme U, Cherevach I, Gong P, Pain A, and Billker O (2010) The systematic functional analysis of Plasmodium protein kinases identifies essential regulators of mosquito transmission. Cell Host Microbe 8 (4), 377–387. [PubMed: 20951971]

(29). Tremp AZ, and Dessens JT (2011) Malaria IMC1 membrane skeleton proteins operate autonomously and participate in motility independently of cell shape. J. Biol. Chem 286 (7), 5383–5391. [PubMed: 21098480]

(30). Kono M, Herrmann S, Loughran NB, Cabrera A, Engelberg K, Lehmann C, Sinha D, Prinz B, Ruch U, Heussler V, Spielmann T, Parkinson J, and Gilberger TW (2012) Evolution and architecture of the inner membrane complex in asexual and sexual stages of the malaria parasite. Mol. Biol. Evol 29 (9), 2113–2132. [PubMed: 22389454]

(31). Harding CR, and Meissner M (2014) The inner membrane complex through development of Toxoplasma gondii and Plasmodium. Cell. Microbiol 16 (5), 632–641. [PubMed: 24612102]

(32). Dixon MW, Dearnley MK, Hanssen E, Gilberger T, and Tilley L (2012) Shape-shifting gametocytes: how and why does P. falciparum go banana-shaped? Trends Parasitol 28 (11), 471–478. [PubMed: 22939181]

(33). Volkmann K, Pfander C, Burstroem C, Ahras M, Goulding D, Rayner JC, Frischknecht F, Billker O, and Brochet M (2012) The alveolin IMC1h is required for normal ookinete and sporozoite motility behaviour and host colonisation in Plasmodium berghei. PLoS One 7 (7), e41409. [PubMed: 22844474]

(34). Keeley A, and Soldati D (2004) The glideosome: a molecular machine powering motility and host-cell invasion by Apicomplexa. Trends Cell Biol 14 (10), 528–532. [PubMed: 15450974]

(35). Baum J, Richard D, Healer J, Rug M, Krnajski Z, Gilberger TW, Green JL, Holder AA, and Cowman AF (2006) A conserved molecular motor drives cell invasion and gliding motility across malaria life cycle stages and other apicomplexan parasites. J. Biol. Chem 281 (8), 5197–5208. [PubMed: 16321976]

(36). Gupta VK, Verma S, Gupta S, Singh A, Pal A, Srivastava SK, Srivastava PK, Singh SC, and Darokar MP (2012) Membrane-damaging potential of natural L-(−)-usnic acid in Staphylococcus aureus. Eur. J. Clin. Microbiol. Infect. Dis 31 (12), 3375–83. [PubMed: 22865029]

(37). Coppens I, and Joiner KA (2003) Host but not parasite cholesterol controls Toxoplasma cell entry by modulating organelle discharge. Mol. Biol. Cell 14 (9), 3804–3820. [PubMed: 12972565]

(38). Johnson TM, Rajfur Z, Jacobson K, and Beckers CJ (2007) Immobilization of the type XIV myosin complex in Toxoplasma gondii. Mol. Biol. Cell 18 (8), 3039–3046. [PubMed: 17538016]

(39). De Miguel N, Lebrun M, Heaslip A, Hu K, Beckers CJ, Matrajt M, Dubremetz JF, and Angel SO (2008) Toxoplasma gondii Hsp20 is a stripe-arranged chaperone-like protein associated with the outer leaflet of the inner membrane complex. Biol. Cell 100(8), 479–489. [PubMed: 18315523]

(40). Di Paolo G, and de Camilli P (2006) Phosphoinositides in cell regulation and membrane dynamics. Nature 443, 651–657. [PubMed: 17035995]

(41). De Napoli MG, de Miguel N, Lebrun M, Moreno SNJ, Angel SO, and Corvi MM (2013) N-terminal palmitoylation is required for Toxoplasma gondii HSP20 inner membrane complex localization. Biochim. Biophys. Acta, Mol. Cell Res 1833 (6), 1329–1337.

(42). Wetzel J, Herrmann S, Swapna LS, Prusty D, Peter ATJ, Kono M, Saini S, Nellimarla S, Wong TW, Wilcke L, Ramsay O, Cabrera A, Biller L, Heincke D, Mossman K, Spielmann T, Ungermann C, Parkinson J, and Gilberger TW (2015) The role of palmitoylation for protein recruitment to the inner membrane complex of the malaria parasite. J. Biol. Chem 290 (3), 1712–1728. [PubMed: 25425642]

(43). Vaughan AM, O'Neill MT, Tarun AS, Camargo N, Phuong TM, Aly ASI, Cowman AF, and Kappe SHI (2009) Type II fatty acid synthesis is essential only for malaria parasite late liver stage development. Cell. Microbiol 11 (3), 506–520. [PubMed: 19068099]

(44). Santos JM, Kehrer J, Franke-Fayard B, Frischknecht F, Janse CJ, and Mair GR (2015) The Plasmodium palmitoyl-S-acyltransferase DHHC2 is essential for ookinete morphogenesis and malaria transmission. Sci. Rep 5, 16034. [PubMed: 26526684]

(45). Lucantoni L, Yerbanga RS, Lupidi G, Pasqualini L, Esposito F, and Habluetzel A (2010) Transmission blocking activity of a standardized neem (Azadirachta indica) seed extract on the rodent malaria parasite Plasmodium berghei in its vector Anopheles stephensi. Malar. J 9, 66. [PubMed: 20196858]

(46). Kumar N, Aikawa M, and Grotendorst C (1985) Plasmodium gallinaceum: critical role for microtubules in the transformation of zygotes into ookinetes. Exp. Parasitol 59 (2), 239–247. [PubMed: 2857655]

(47). Jones IW, Denholm AA, Ley SV, Lovell H, Wood A, and Sinden RE (1994) Sexual development of malaria parasites is inhibited in vitro by the neem extract azadirachtin, and its semi-synthetic analogues. FEMS Microbiol. Lett 120 (3), 267–273. [PubMed: 7980823]

(48). Miguel-Blanco C, Lelièvre, Delves MJ, Bardera AI, Presa JL, López-Barragán MJ, Ruecker A, Marques S, Sinden RE, and Herreros E (2015) Imaging-based high-throughput screening assay to identify new molecules with transmission-blocking potential against Plasmodium falciparum female gamete formation. Antimicrob. Agents Chemother 59 (6), 3298–3305. [PubMed: 25801574]

(49). Dinglasan RR, Kalume DE, Kanzok SM, Ghosh AK, Muratova O, Pandey A, and Jacobs-Lorena M (2007) Disruption of Plasmodium falciparum development by antibodies against a conserved mosquito midgut antigen. Proc. Natl. Acad. Sci. U. S. A 104 (33), 13461–13466. [PubMed: 17673553]

(50). Dinglasan RR, Alaganan A, Ghosh AK, Saito A, van Kuppevelt TH, and Jacobs-Lorena M (2007) Plasmodium falciparum ookinetes require mosquito midgut chondroitin sulfate proteoglycans for cell invasion. Proc. Natl. Acad. Sci. U. S. A 104 (40), 15882–15887. [PubMed: 17873063]

(51). Ramakrishnan C, Delves MJ, Lal K, Blagborough AM, Butcher G, Baker KW, and Sinden RE (2012) Laboratory maintenance of rodent malaria parasites. Methods Mol. Biol 923, 51–72.

(52). Vlachou D, Zimmermann T, Cantera R, Janse CJ, Waters AP, and Kafatos FC (2004) Real-time, in vivo analysis of malaria ookinete locomotion and mosquito midgut invasion. Cell. Microbiol 6(7), 671–685. [PubMed: 15186403]

(53). Duffy S, and Avery VM (2013) Identification of inhibitors of Plasmodium falciparum gametocyte development. Malar. J 12, 408. [PubMed: 24206914]

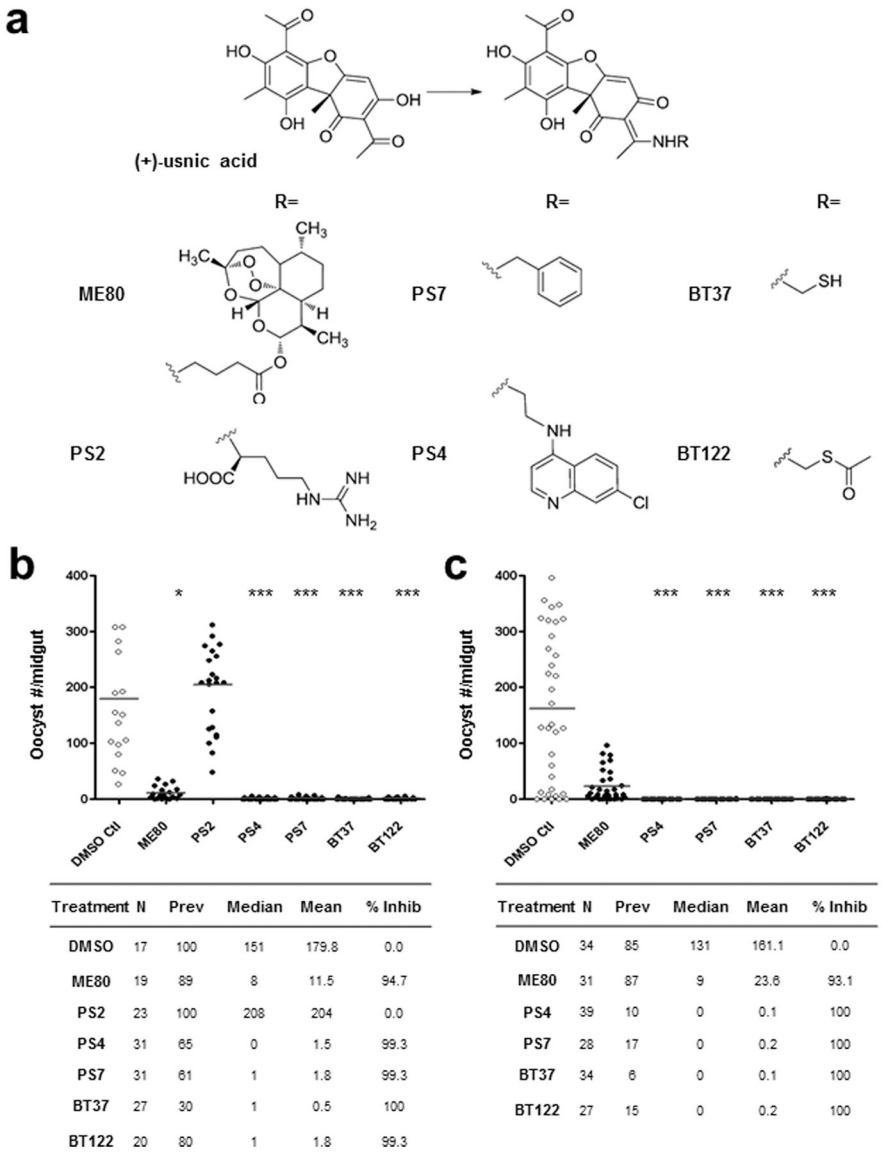

Treatment	N	Prev	Median	Mean	% Inhib
DMSO	17	100	151	179.8	0.0
ME80	19	89	8	11.5	94.7
PS2	23	100	208	204	0.0
PS4	31	65	0	1.5	99.3
PS7	31	61	1	1.8	99.3
BT37	27	30	1	0.5	100
BT122	20	80	1	1.8	99.3

Treatment	N	Prev	Median	Mean	% Inhib
DMSO	34	85	131	161.1	0.0
ME80	31	87	9	23.6	93.1
PS4	39	10	0	0.1	100
PS7	28	17	0	0.2	100
BT37	34	6	0	0.1	100
BT122	27	15	0	0.2	100

Figure 1.

Initial screening of usnic acid derivatives for transmission-blocking activity demonstrating reduced midgut-infection intensity. (a) Structure of usnic acid (UA) and the UA derivatives initially screened by standard membrane feeding assay (SMFA). For each derivative the UA scaffold remains the same, and R represents the point of attachment for each functional group. (b, c) Initial screening of UA derivatives by SMFA carried out at a concentration of 250 μg/mL. The readout for midgut infection is oocyst intensity, plotted as the number of oocysts per female mosquito. DMSO-only treatments were included as negative controls. Experimental details are tabulated below the graphs, where *N* is the number of mosquito midguts dissected and scored for oocysts, “prev” is the infection prevalence among mosquitoes in a given treatment group with the 95% confidence interval provided in parentheses beneath the observed value, mean is the geometric mean of oocyst number (includes nonzero midguts only), median is the median oocyst number, and % inhibition is

calculated as ($median_{control} - median_{treatment}$)/$median_{control}$. The level of statistical significance is denoted by asterisks following Bonferroni correction of *z*-scores, *$p < 0.05$, ***$p < 0.0001$.

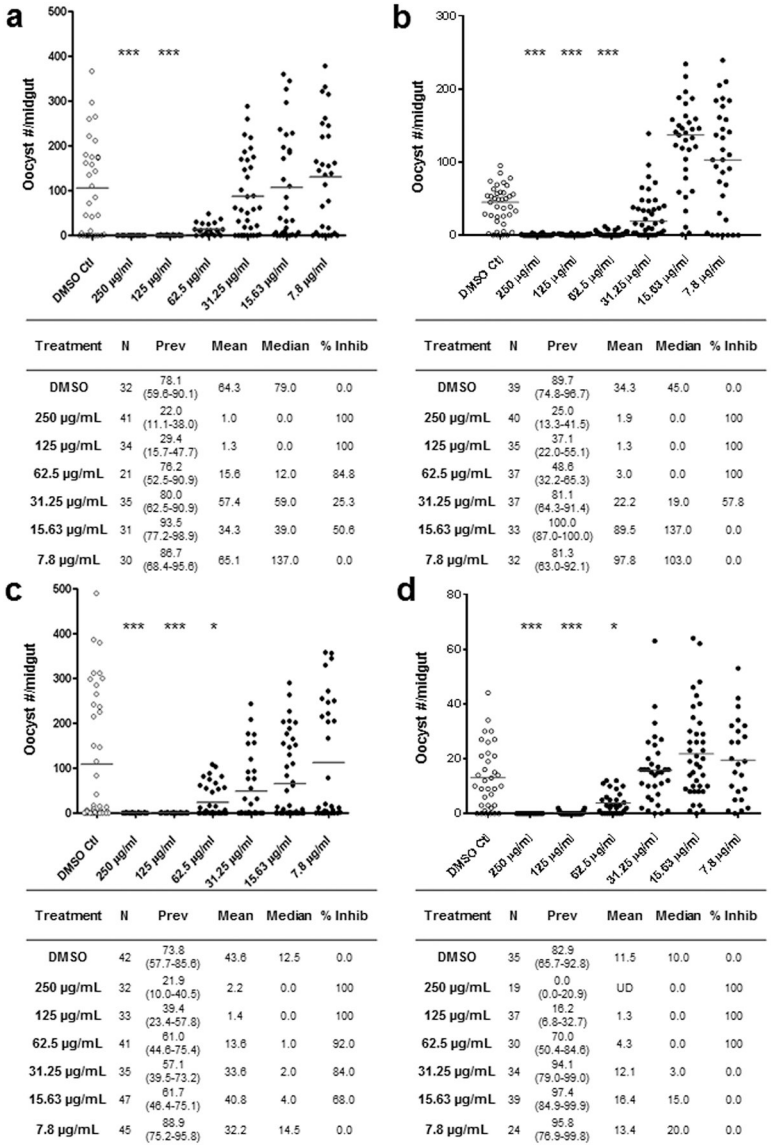

Treatment	N	Prev	Mean	Median	% Inhib
DMSO	32	78.1 (59.6-90.1)	64.3	79.0	0.0
250 µg/mL	41	22.0 (11.1-38.0)	1.0	0.0	100
125 µg/mL	34	29.4 (15.7-47.7)	1.3	0.0	100
62.5 µg/mL	21	76.2 (52.5-90.9)	15.6	12.0	84.8
31.25 µg/mL	35	80.0 (62.5-90.9)	57.4	59.0	25.3
15.63 µg/mL	31	93.5 (77.2-98.9)	34.3	39.0	50.6
7.8 µg/mL	30	86.7 (68.4-95.6)	65.1	137.0	0.0

Treatment	N	Prev	Mean	Median	% Inhib
DMSO	39	89.7 (74.8-96.7)	34.3	45.0	0.0
250 µg/mL	40	25.0 (13.3-41.5)	1.9	0.0	100
125 µg/mL	35	37.1 (22.0-55.1)	1.3	0.0	100
62.5 µg/mL	37	48.6 (32.2-65.3)	3.0	0.0	100
31.25 µg/mL	37	81.1 (64.3-91.4)	22.2	19.0	57.8
15.63 µg/mL	33	100.0 (87.0-100.0)	89.5	137.0	0.0
7.8 µg/mL	32	81.3 (63.0-92.1)	97.8	103.0	0.0

Treatment	N	Prev	Mean	Median	% Inhib
DMSO	42	73.8 (57.7-85.6)	43.8	12.5	0.0
250 µg/mL	32	21.9 (10.0-40.5)	2.2	0.0	100
125 µg/mL	33	39.4 (23.4-57.8)	1.4	0.0	100
62.5 µg/mL	41	61.0 (44.6-75.4)	13.6	1.0	92.0
31.25 µg/mL	35	57.1 (39.5-73.2)	33.6	2.0	84.0
15.63 µg/mL	47	61.7 (46.4-75.1)	40.8	4.0	68.0
7.8 µg/mL	45	88.9 (75.2-95.8)	32.2	14.5	0.0

Treatment	N	Prev	Mean	Median	% Inhib
DMSO	35	82.9 (65.7-92.8)	11.5	10.0	0.0
250 µg/mL	19	0.0 (0.0-20.9)	UD	0.0	100
125 µg/mL	37	16.2 (6.8-32.7)	1.3	0.0	100
62.5 µg/mL	30	70.0 (50.4-84.6)	4.3	0.0	100
31.25 µg/mL	34	94.1 (79.0-99.0)	12.1	3.0	0.0
15.63 µg/mL	39	97.4 (84.9-99.9)	16.4	15.0	0.0
7.8 µg/mL	24	95.8 (76.9-99.8)	13.4	20.0	0.0

Figure 2.

Usnic acid derivatives exhibiting dose−response relationships with *Plasmodium*-infection intensity in the mosquito midgut. Two replicates of dose–response SMFAs are shown for each UA derivative, (a,b) BT37 and (c,d) BT122. For each compound, a 2-fold dilution series was performed in DMSO prior to mixing with gametocyte-infected erythrocytes. The column headings in tables below each graph and the levels of statistical significance are indicated as in Figure 1.

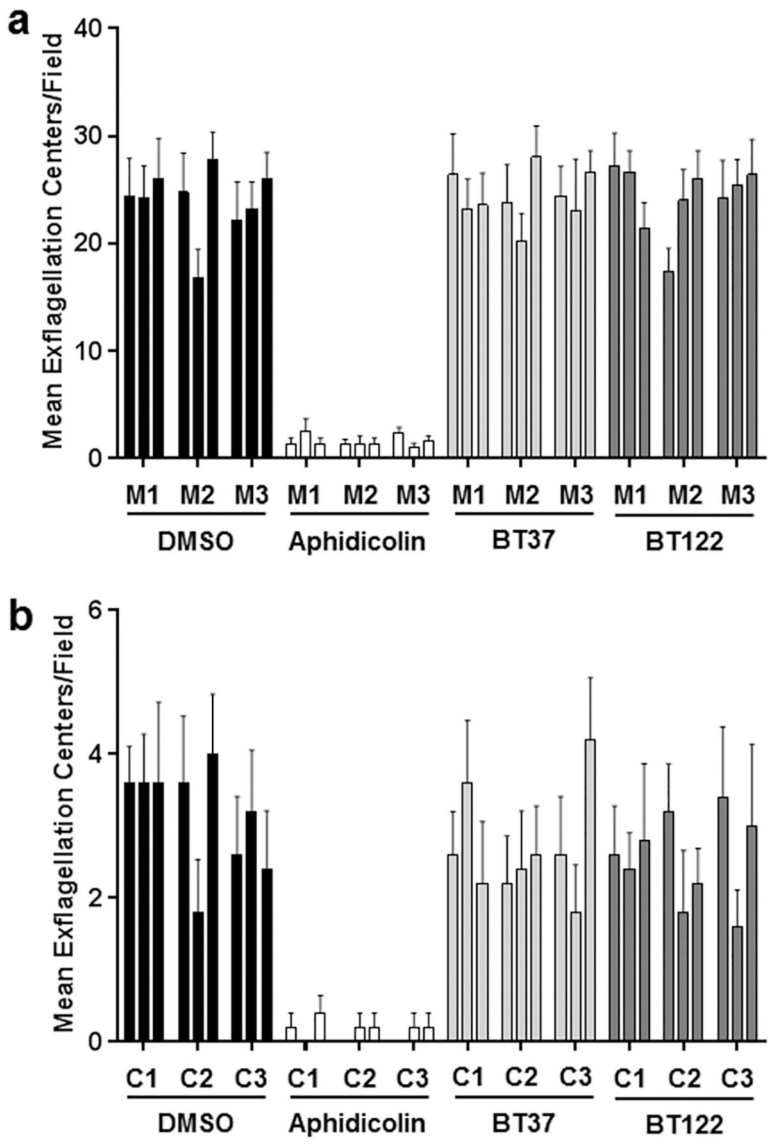

Figure 3.

Treatment of *Plasmodium* cultures with UA derivatives with no effect on microgametogenesis. (a) Blood from mice infected with *P. berghei* ANKA was mixed with DMSO, aphidicolin, BT37, or BT122 in ookinete media, incubated for 15 min, and then analyzed by microscopy for exflagellation. For each treatment group, the number of exflagellation centers was scored for five fields per replicate and three replicates per mouse (M1–M3). The arithmetic means for all replicates are reported. (b) For *P. falciparum* (NF54), the same assay was performed using gametocyte cultures (C1–C3) instead of mice. As in a, arithmetic means are reported for all replicates.

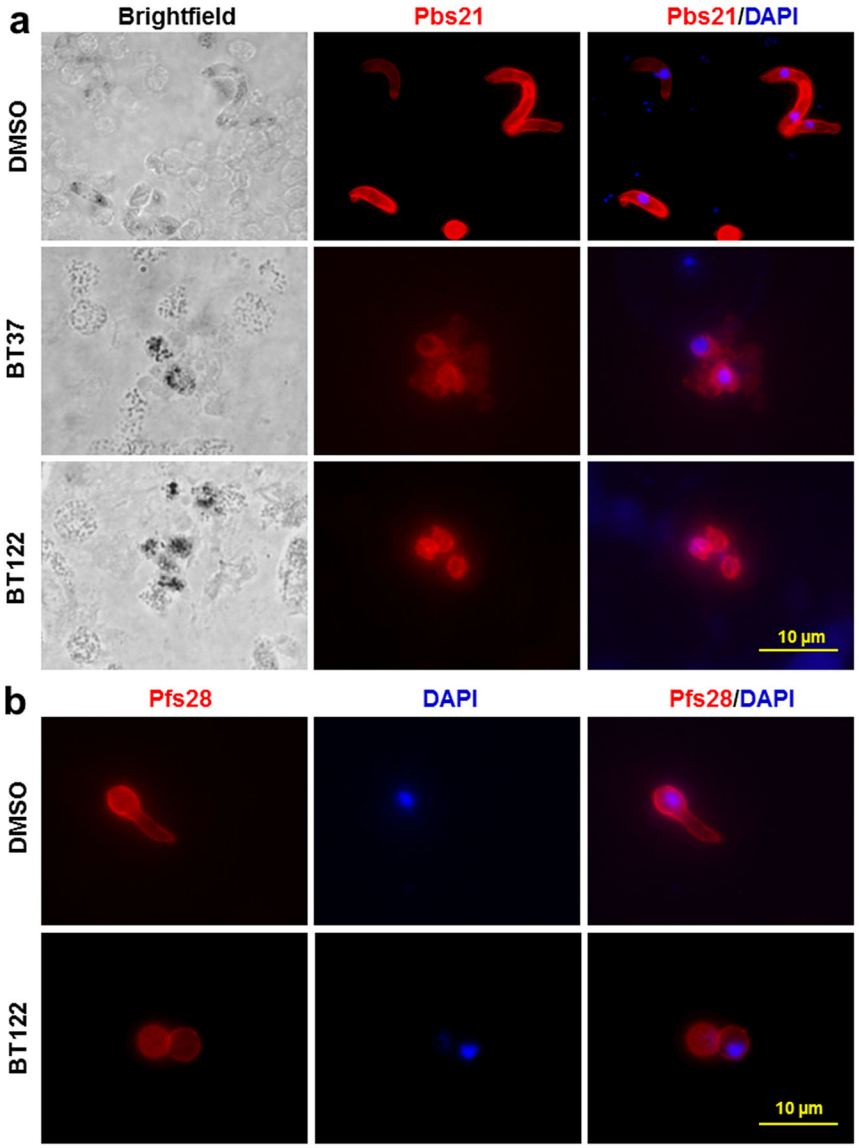

Figure 4.

Treatment of *Plasmodium* cultures with UA derivatives inhibits normal ookinete development. (a) *P. berghei* ANKA parasites from both treatment and control cultures were labeled with anti-Pbs21 antibody to evaluate the effect of UA derivatives (250 μg/mL) on ookinete development. DMSO-control group ookinetes showed the characteristic elongated shape typical of normal development after 24 h. In contrast, ookinete cultures at 24 h exposed to either BT37 or BT122 showed the presence of small round cells that expressed Pbs21 but failed to transform into elongated ookinetes. (b) Similar results were found for *P. falciparum* ookinete development in blood meals dissected form mosquito midguts 24 h post feeding. Mosquitoes fed infectious blood meals with DMSO alone show retorts in the process of elongation at 24 h, while those fed blood and gametocytes with BT122 showed impaired development inside A. *gambiae* mosquitoes at 24 h post blood feeding. Scale bar = ~10 μm.

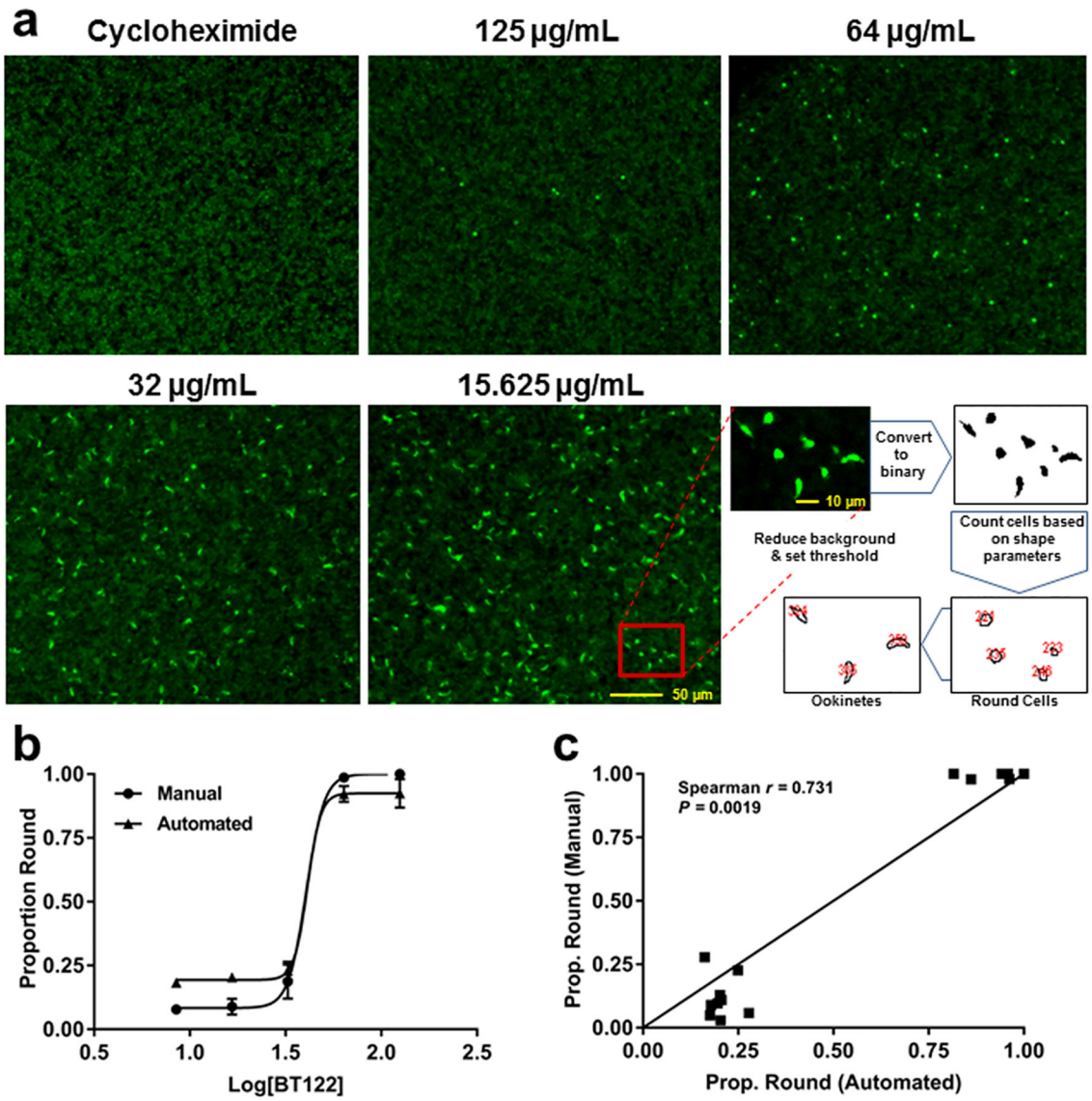

Figure 5.

Automated counts of ookinetes and round cells yield similar proportions as manual counts. (a) Representative images from ookinete-development assays with *P. berghei* CTRP-GFP and a schematic showing how the automated counting program distinguishes between ookinetes and round cells. Cycloheximide was used as a positive control (loss of ookinete development) to determine background fluorescence. (b) Proportion of round cells plotted against concentration of BT122 on a log scale for both manual (circles) and automated (triangles) counts. Note that logistic curves fit to each data set yielded similar best-fit values for the Hill slope, 9.23 for manual (R^2 = 0.9879) and 12.54 (R^2 = 0.9827) for automated. (c) Proportion of round cells from manual vs automated counts of the same wells across three replicates (15 wells total) plotted against one another. A direct positive correlation would result in points falling on the line (slope = 1.0). The Spearman nonparametric test for correlation rejected the null hypothesis of no correlation between the methods. Taken

together, the data in both panels suggest that automation reasonably approximates counting by eye but with opposite biases at each extreme. At high concentrations of BT122, automation tends to count a handful of false positive ookinetes, slightly reducing the proportion of round cells. At low concentrations of BT122, the program tends to overestimate the proportion of round cells due mostly to clumping of ookinetes or retorts that are counted as single parasites.

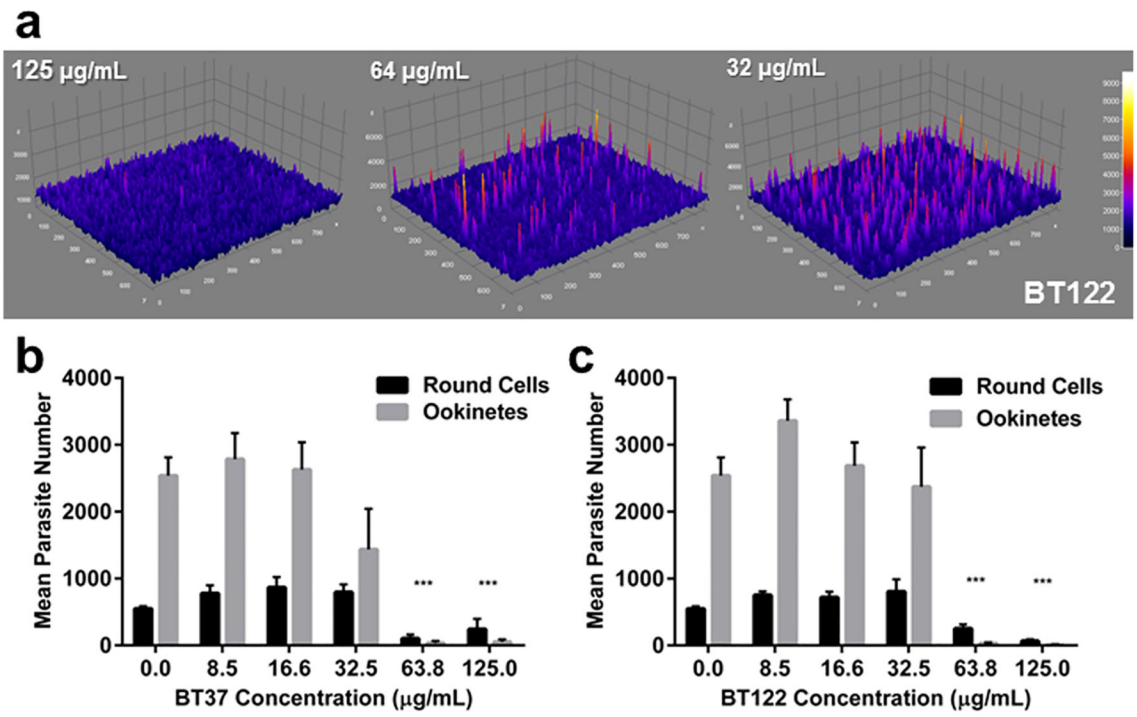

Figure 6.

UA derivatives impair ookinete development in *P. berghei* cultured *in vitro*. (a) Three-dimensioinal surface plots showing variation in GFP fluorescence intensity associated with a dose of BT122. (b) Relationship between dose of BT37 and the mean number of fluorescing parasites distinguished by shape (ookinetes or round cells). To be conservative, shape parameters for the ookinete category were optimized to capture retorts and immature ookinetes since development was not fully impaired in these parasites. Means and standard errors were calculated from counts of four replicates per concentration. (c) Same as panel b for BT122.